PROCEEDINGS OF ISAP '96, CHIBA, JAPAN

ELECTROMAGNETIC ANALYSIS OF X-RAY FOCUSSING DEVICES USING BEAM PROPAGATION METHOD

Yasumitsu MIYAZAKI and Takashi OKUYAMA
Toyohashi University of Technology, Tempaku-cho. Toyohashi-shi, Aichi, 441 Japan.

1 Introduction

Recently in the field of x-ray applications many types of functional devices that need compact design have become necessary. x-ray focussing devices can be divided into diffraction and total reflection types. but those based on refraction have not been well discussed until now.In this study, we consider functional devices for focussing x-rays. At first x-ray focussing is examined by using ray tracing method based on geometrical optics. Here we propose x-ray focussing devices based on distributed refractive index medium. Then Beam Propagation Method is utilized to investigate the properties of propagating x-rays in a distributed index medium. Furthermore, a loss term is introduced into Beam Propagation Method and propagation loss with regard to core thickness is analysed.

2 Analysis method

We treat monochromatic wave propagation in 3D isotropic material using Beam Propagation Method. Because that problem can be mathematically converted by virtue of effective refractive index, in this paper, x-ray through a 2D medium would be considered.

Each component of electromagnetic wave (E, H) satisfies a scalar *Helmholtz* equation.

$$\left(\frac{\partial^2}{\partial x^2}+\frac{\partial^2}{\partial z^2}\right)X(x,z)+k_0^2N^2(x,z)X(x,z)=0 \tag{1}$$

where $N(x,z)$ is the effective index.

$X(x,z)$ can be represented by using another complex amplitude $W(x,z)$ and standard velocity factor as follows.

$$X(x,z)=W(x,z)\exp[-jk_0N_0z] \tag{2}$$

$$W(x,z+\Delta z)=\exp\left\{-j\Delta z\left[\frac{\nabla_t^2}{(\nabla_t^2+k_0^2N_0^2)^{1/2}+k_0N_0}+\chi(x,z)\right]\right\}W(x,z) \tag{3}$$

$$\chi(x,z)=k_0\delta N(x,z) \tag{4}$$

Here we use a ***Baker-Hausdorff*** theory with respect to non-commutative operator $\hat{\mathbf{A}}, \hat{\mathbf{B}}$ and split the first term on right-hand side of eqn.(3) as $\exp(\Delta z\hat{\mathbf{A}}+\Delta z\hat{\mathbf{B}})\approx\exp(\Delta z\hat{\mathbf{A}})\exp(\Delta z\hat{\mathbf{B}})$, thus eqn.(3) becomes,

$$\begin{aligned}W(x,z+\Delta z) &= \exp\left\{-j\frac{\Delta z}{2}\left[\frac{\nabla_t^2}{(\nabla_t^2+k_0^2N_0^2)^{1/2}+k_0N_0}\right]\right\}\times\exp[-j\Delta z\chi(x,z)]\\ &\quad\times\exp\left\{-j\frac{\Delta z}{2}\left[\frac{\nabla_t^2}{(\nabla_t^2+k_0^2N_0^2)^{1/2}+k_0N_0}\right]\right\}W(x,z)+O(\Delta z^3)\end{aligned} \tag{5}$$

2.1 Consideration of propagation loss

The refractive index in x-ray region is generally represented as

$$n=1-\delta-j\beta \tag{6}$$

But, we describe the refractive index as follows to avoid confusion in the phase constant.

$$n = n_r - jn_i \tag{7}$$

The propagation constants γ_c, k_y, γ_s are represented using effective refractive index and medium constants in each area, clad, core and substrate,

$$\gamma_c = k_0\sqrt{N^2 - n_c^2},\ k_y = k_0\sqrt{n_f^2 - N^2},\ \gamma_s = k_0\sqrt{N^2 - n_s^2} \tag{8}$$

$$k_yT = (m+1)\pi - \tan^{-1}\left(\frac{k_y}{\gamma_s}\right) - \tan^{-1}\left(\frac{k_y}{\gamma_c}\right) \tag{9}$$

Suppose that x-rays are strongly guided in core region, then

$$n_f - N \ll N - n_s \tag{10}$$

Under this condition, eigen equation (9) including two terms of $\tan^{-1}$ can be approximated and rewritten as

$$k_y = \frac{(m+1)\pi}{T}\frac{1}{1+\frac{1}{\gamma_s T}+\frac{1}{\gamma_c T}} \tag{11}$$

Since x-rays are incident at grazing incidence of milli-radian order, a high reflectivity (total reflection) may be gained, and we can assume that the incidence is nearly along the propagating direction ($\theta \sim \pi/2$). Thus we can express k_z as

$$k_z \approx k_0 n_f\left[1 - \frac{1}{2}\left(\frac{k_y}{k_0 n_f}\right)^2\right] \tag{12}$$

We can define z direction wave number with loss as

$$k_z = \beta - j\alpha \qquad (\alpha > 0) \tag{13}$$

Here we suppose that propagation loss is small in view of the assumption that the mode is strongly guided. Therefore, β and α are expressed as

$$\beta = k_0 n_f - \frac{1}{2k_0 n_f}\left\{\frac{(m+1)\pi}{T}\right\}^2\left(1 - \frac{2Re(\gamma_s)}{|\gamma_s|^2 T} - \frac{2Re(\gamma_c)}{|\gamma_c|^2 T}\right) \tag{14}$$

$$\alpha \simeq \frac{1}{\beta}\frac{\{(m+1)\pi\}^2}{T^3}\left[\frac{Im(\gamma_s)}{|\gamma_s|^2} + \frac{Im(\gamma_c)}{|\gamma_c|^2}\right] \tag{15}$$

Since the propagation equation (5) corresponds to a periodic lens array in a homogeneous medium, a phase correction can be built into a eqn (15).

3 Numerical analysis

To realize an x-ray focussing device, we propose a structure as shown in Fig.2. The materials

Table 1. Materials (at $\lambda = 11.4[nm]$)

region	substance	n_r	n_i
core(inside)	C	0.973174	0.003919
core(outside)	Rh	0.927401	0.004413
clad,substrate	Au	0.925128	0.029784

of such device are chosen according to the following conditions:

1. Core region (a) Refractive index to be greater than clad and substrate. (b) To have large variation of core index. (c) To have low loss.

2. Clad and substrate region (a) Refractive index to be smaller than core. (b) Choosen to have a greater loss.

With these conditions, we choose each material as displayed in Table 1. The refractive indices are calculated using scattering data obtained experimentally in [2].

$$g(x) = \frac{erf[(x+T_0/2)/d_x] - erf[(x-T_0/2)/d_x]}{2erf(T_0/2d_x)}, DT \equiv (T_0/d_x) \tag{16}$$

Here T_0 is pattern width before diffusion and d_x is the depth of diffusion.

We discuss here how the proper incident beam width was obtained by changing core layer distribution width. The ratio of beam width w_0 to distribution width (depth of diffusion d_x in Eqn.(16)) is defined as

$$k \equiv DT/w_0. \tag{17}$$

By varying the incident x-ray beam width (w_0 : 20, 50, and 100 nm), we calculate the beam focussing ratio $w(z)/w_0$.

Fig.3 shows the variation of spot size with propagation distance for various values of k as a parameter. We find focussing action for $k \leq 1.0$. Fig.4~5 shows a similar result for different beam widths. We find discontinuities in the curves for $w_0 = 100nm$, which can be explained as due to the excitation of higher order modes.

Based on the above results, suitable core layer distribution width is found to be $DT = 2w_0$. For each beam width, the magnification is proportional to focussing distance as shown in Fig.6. This result allows the design of a focussing device for a given x-ray beam width.

Using the results we investigate a focussing device of length $40nm$ ($DT = 100nm, T = 50nm$) using a gaussian pulse of beam width $50nm$. We observe that the beam to be focussed at a distance of $21.5nm$.(Fig.7) This is when the refractive index is real.

Including an imaginary part for the refractive index profile we repeat the computation and the results are shown in Fig.8.

4 Conclusion

In this study, the properties of x-ray focussing devices are analyzed by using Beam Propagation Method. The characteristics of x-rays for an error function type distribution medium are calculated. The following calculations are done: (1) Distribution width for incident beam width. (2) Proper device length for incident beam width. (3) After assuming the loss factor, we observed that the output intensity at the focus has been reduced.

References

[1] Terrence Jach, M.J.Chester and S.M.Thurgate, Sci. Instrum., 65, (2), pp.339-342(1994).

[2] B.L.Henke, P.Lee, T.J.Tanaka, R.L.Shimabukuro, B.K.F.Fujikawa, vol.27, No.1, pp.22-115(1982).

[3] M.D.Feit and J.A.Fleck,Jr., Appl. Opts, vol 17, 24, pp.3990-3998(1978).

[4] M.D.Feit and J.A.Fleck,Jr., Appl. Opts, vol.19, 13, pp.2240-2246(1980).

[5] Y.Miyazaki and R.Ogawa, Progress in Electromagnetics Research Symp, MIT, S5A5, 7, pp682(1991)

[6] Y.Miyazaki, R.Ogawa and H.Kobayashi, Proc. of Int. Symp. Antennas and Propagation (ISAP'92), Sapporo, pp57-60 (1992)

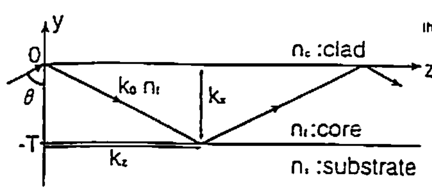

Fig.1 Wave number relationship

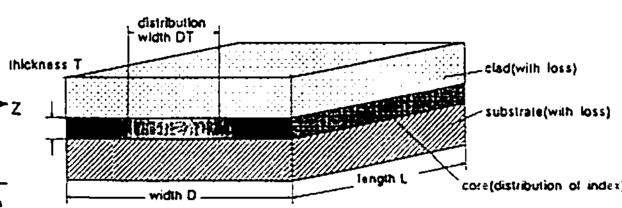

Fig.2 X-ray focusing device structure

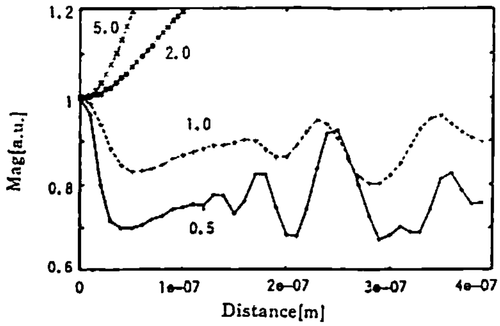

Fig.3 Beam width (at w_o = 20 nm)

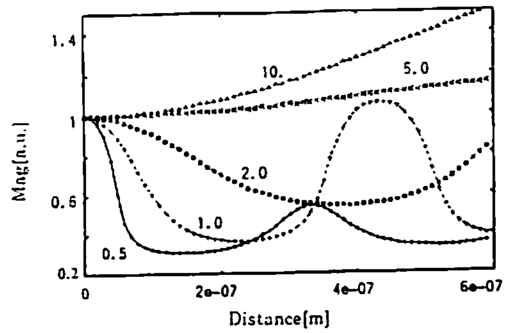

Fig.4 Beam width (at w_o = 50 nm)

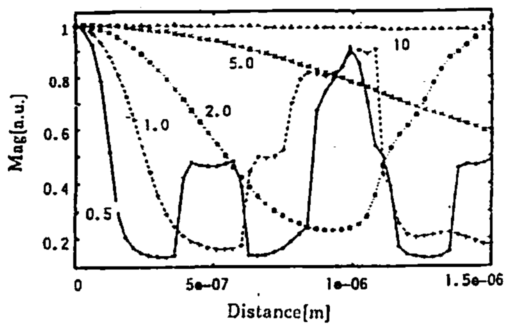

Fig.5 Beam width (at w_o = 100 nm)

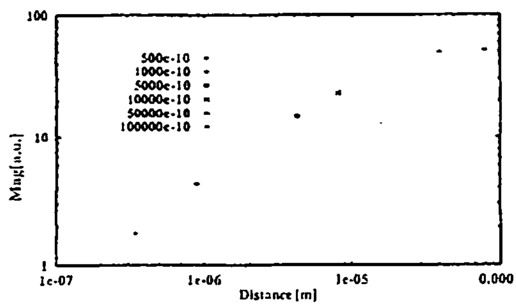

Fig.6 Magnification of Beam

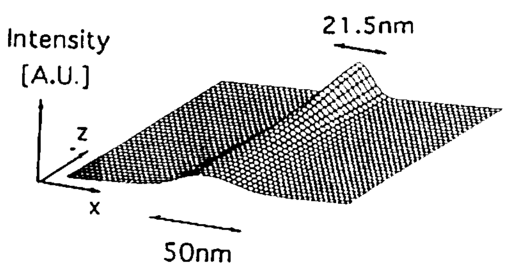

Fig.7 Focusing property of lossless waveguide

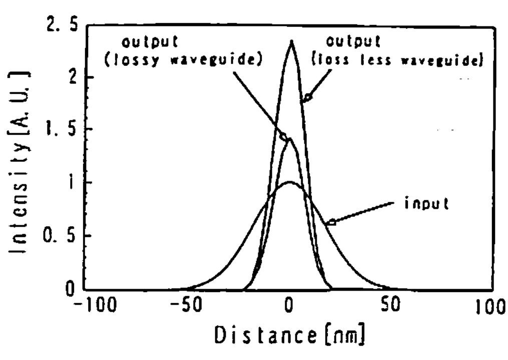

Fig.8 Comparison of foucusing properties.